Observation of matter wave beat phenomena in the macrodomain for electrons moving along a magnetic field

Ram K. Varma, A. M. Punithavelu, and S. B. Banerjee
Physical Research Laboratory, Ahmedabad 380 009, India

(Received 23 May 2001; revised manuscript received 16 August 2001; published 25 January 2002)

We report here the observations that exhibit the existence of matter wave phenomena with wavelength in the macrodomain of a few centimeters, for electrons moving along a magnetic field from an electron gun to a collector plate situated behind a grounded grid. These are in accordance with the predictions of a quantumlike theory for charged particles in the classical macrodomain, given by one of the authors [R. K. Varma, Phys. Rev. A **31**, 3951 (1985)] with a recent generalization [R. K. Varma, Phys. Rev. E **64**, 036608 (2001)]. The beats correspond to two closely spaced ''frequencies'' in the system, with the beat frequency given, in accordance with the characteristics of a wave phenomena, by the difference between the two frequencies. The beats ride as a modulation over a discrete energy band structure obtained with only one frequency present. The frequency here corresponds to the distance between the electron gun and the detector plate as it characterizes the variation in the energy band structure as the electron energy is swept. The second ''frequency'' corresponds to the gun-grid distance. These observations of the beats of matter waves in this experiment, with characteristics in accordance with the wave algorithm, then establish unambiguously the existence of macroscopic matter waves for electrons propagating along a magnetic field.

DOI: 10.1103/PhysRevE.65.026503 PACS number(s): 41.75.−i, 41.85.−p, 41.90.+e, 03.65.Ta

I. INTRODUCTION

In a recent paper one of the authors (Varma [1]) has derived a set of Schrödinger-like equations for charged particles propagating along a magnetic field. Just like the QM-Schrödinger equation, these are equations for the probability amplitudes $\Psi(n)$,

$$\frac{i\mu}{n}\frac{\partial\Psi(n)}{\partial t}=-\left(\frac{\mu}{n}\right)^2\frac{\partial^2\Psi(n)}{\partial x^2}+(\mu\Omega)\Psi(n),\quad n=1,2,3,..., \tag{1}$$

along with the expression for the probability density given by

$$\mathcal{P}(x,t)=\sum_n \Psi^*(n)\Psi(n), \tag{2}$$

and are obtained in Ref. [1] in the correspondence limit starting from the QM-Schrödinger equation in its path integral representation. Consequently they apply in the classical mechanical parameter domain or the clasical macrodomain and their amplitude character flows directly from that of Schrödinger wave equation. They are one dimensional in the coordinate x along the magnetic field line. These equations were also obtained earlier by Varma [2] from the classical Liouville equation as its Hilbert-space representation, and the matter wave phenomena predicted therefrom in the macrodomain. Though this derivation is quite interesting and instructive, the advantage of the quantum mechanical derivation is that the amplitude character of the derived equations has an unreserved validity.

The μ in these equations is the gyroaction for the charged particles motion around the magnetic field line, $\mu=1/2mv_\perp^2/\Omega$ [$v_\perp$ is the component of the velocity perpendicular to the magnetic field, $\Omega=eB/mc$ is the gyrofrequency in the magnetic field B], and $(\mu\Omega)$ is the ''adiabatic potential'' that describes the reduced motion of the particle along the magnetic field when μ is an adiabatic invariant (see, for instance, Northrop [3]).

It will be seen that μ appears in the role of $\hbar$ in these Schrödinger-like equations [1]. As discussed in Ref. [1], quantum mechanically, μ is identified as $\mu\equiv\nu\hbar$, with $\nu\gg1$, being a large Landau level quantum number in the correspondence limit; μ is then an action with a macroscopic magnitude, being typically $\mu\approx10^8\hbar$, in the typical laboratory situations. (For an electron energy $\mathcal{E}=1$ keV, and magnetic field $B=100$ G, $\mu\approx10^{-18}$ erg s, which is $\sim10^8\hbar$). Of course, μ is not any fundamental constant like the $\hbar$ in the Schrödinger wave equation, and is actually identified as the initial value at injection in an experiment.

In view of the macroscopic magnitude of the action μ, Eq. (1) along with the connection (2) for the probability density, predict the existence of matter wave phenomena with macroscopic wavelength $\lambda_M\approx10^8-10^9$ Å $=1-10$ cm.

From Eq. (1) the wave function for a free particle has the form $\Psi(1)=\exp(ip_\parallel x/\mu)$, for the mode number $n=1$. However, since the injected μ may have a small spread $\delta\mu$ around a mean $\overline{\mu}$, an integration of $\Psi(1)$ over this distribution yields an effective wave function of the form $\exp[i\Omega x/v_\parallel]$. This implies a wavelength of the form, $\lambda_M=2\pi v_\parallel/\Omega$, which is independent of $\hbar$, and of macroscopic dimensions. For a magnetic field $B\approx100$ G, and an electron velocity $v\approx10^9$ cm s^{-1}, $\lambda_M\approx4$ cm. This is clearly of macroscopic magnitude as against the magnitude of typical de Broglie wavelength of a few angstrom. There is, however, also a more direct quantum mechanical demonstration of the macroscopic form of the wave function, $\exp(i\Omega x/v_\parallel)$. It is given here in the Appendix to afford a greater conviction.

The existence of matter waves with wavelength of macroscopic dimensions ~5 cm for the charged particles along

magnetic fields, as predicted by these equations is a rather novel and extraordinary proposition. Such matter waves with macroscopic wavelengths have not been proposed prior to the considerations and consequences arising out of the theories of Refs. [1], [2]. An experimental check of these predictions should be quite fascinating to perform.

Experiments have been carried out earlier [4] on the transmission of electrons along magnetic field with the sweeping of the potential on the biased grid of the detector, as the electrons of a given energy from an electron gun traverse to the detector along the magnetic field. The observed plate and grid currents as a function of the bias voltage on the detector grid exhibited a series of sharply defined maxima and minima that were entirely contrary to the expectation from the Lorentz equation of motion, according to which one expects to obtain a standard ''retarding potential analyzer'' (RPA) response. These observed maxima and minima were concluded to be indicative of the existence of matter wave phenomena alluded to above.

However, it turns out that the experimental methodology used in these experiments was a little more complex than necessary, resulting in more than one beam a primary and a secondary one (arising from secondary electrons). Because of this circumstance the observed maxima and minima lend themselves to the possibility of an alternative interpretation [5] as has also been suggested by Ito and Yoshida [6], who have observed maxima and minima similarly to our observations [4], but have advanced an alterative mechanism, involving basically the properties of the particle trajectories. It must be added, however, that by the authors' own concluding remarks [6], the numerical simulation based on their proposed mechanism is unable to reproduce the depth of the modulation observed by them. So it seems reasonable to identify the modulation in their experiment a manifestation of interference maxima and minima, in accordance with the wave property.

From the above discussion it is clear that while the experiments [4] carried out so far to check the existence of the matter waves in the macrodomain (for charged particles in a magnetic field) do indicate their manifestation, it is imperative to produce a much tighter experimental evidence in favor of the matter wave manifestation, which would have no possibility of being reproduced in terms of the classical particle dynamics in the magnetic field.

One such wave property is the beat phenomena in waves. It is well known that in a wave phenomena, the beat frequency ω_B is given by the difference between the two beating frequencies $\omega_B = \omega_1 - \omega_2$, where $\omega_B \ll \omega_1, \omega_2$. This follows for the intensity of the superposed waves, which is obtained as the magnitude squared of the superposed amplitudes. This is an essential and characteristic wave property. A demonstration of this property for a phenomenon would unambiguously establish its credence as a wave phenomenon.

We wish to present in this paper experimental evidence for the existence of beats with the system under consideration, which are shown to have a ''frequency'' which is equal to the difference between the two closely spaced ''frequencies.'' We shall see later what is meant by a frequency in the context of the experiment. The observation of ''beats'' with the required beat frequency would thus constitute a crucial test of the validity of the matter wave picture in the macrodomain as propounded in the above mentioned theory [1,2].

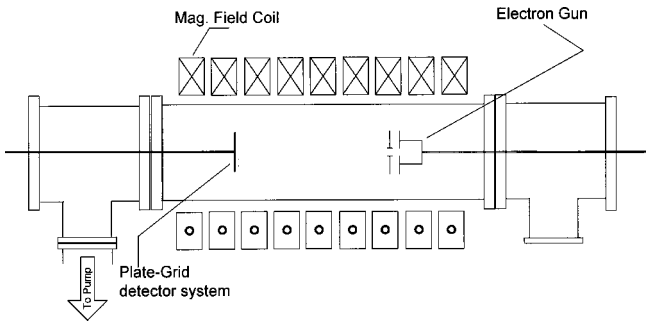

FIG. 1. Schematic diagram of the experimental device.

We describe in the next section (Sec. II) the experiment and present its results that exhibit the existence of beats. In Sec. III, we present an analysis of the experimental data, and in Sec. IV the wave algorithm based on the theory [1,2] as applied to the present experiment. This shows how in this experiment the beat frequency, as the difference between the two closely spaced frequencies would follow only when, following the standard wave picture, the intensity is related to the square of the amplitude.

II. THE EXPERIMENT

The experiment is carried out by studying the transmission characteristics of a stream of charged particles (electrons) along a magnetic field from an electron gun to a detector plate. The stream is taken to be of such a low intensity ($\sim$nA) that it can be regarded as consisting of only individual particles without any interparticle collisions or collective effects. (For an energy of electrons $\mathcal{E} \sim 1$ keV a nanoampere current corresponds to a linear electron number density of approximately 10 cm^{-1}, and volume number density $\approx n_e \sim 10^2\ \mathrm{cm}^{-3}$, taking the diameter of the electron stream to be $\sim$2 mm. This is quite a low number density that makes the interparticle collisions inconsequential and collective effects absent).

The experimental chamber consists of a glass cylinder (length 85 cm, diameter 11 cm), which is evacuated to $\sim 4 \times 10^{-6}$ Torr. The magnetic field is produced by a set of solenoid coils fed by a low-voltage high-current power supply, and can be varied, if desired, by varying the current in the coils. The electrons are injected almost parallel to the magnetic field (very small pitch angle $\delta \leqslant 5°$) from an electron gun placed at one end of the chamber. At the other end is placed a detector, a flat grounded stainless steel (SS) plate, behind a grounded SS grid [Fig. 1]. The plate is kept at a fixed distance from the gun anode, but the grid is made movable with the help of a Wilson feedthrough. The plate-gun distance can also be varied if desired.

The experiment is carried out by sweeping the cathode voltage of the electron gun, so as to vary the electron energy, and recording both the plate and the grid currents as a function of the cathode voltage (electron energy). The experiment is repeated after varying the distance between the plate and

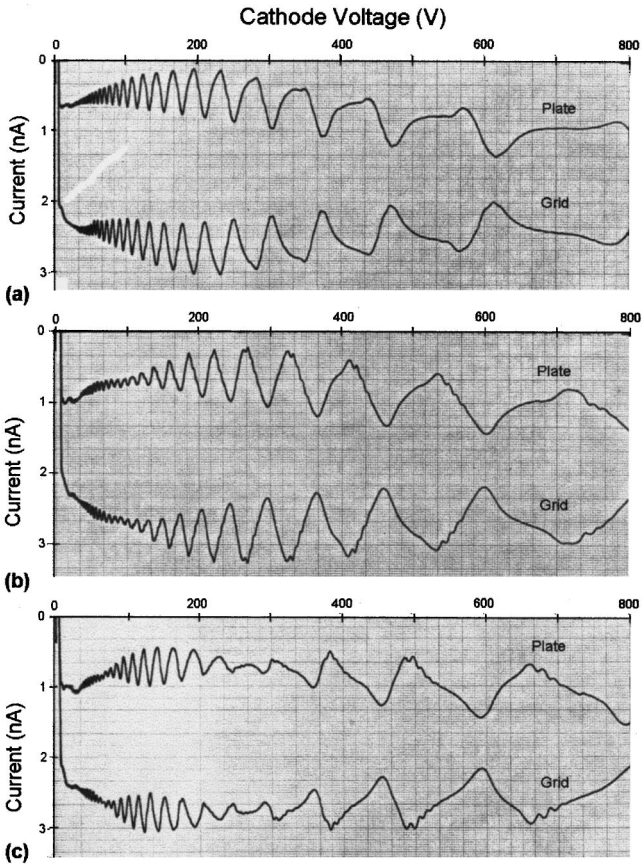

FIG. 2. Plate and grid current plots as a function of cathode voltage (electron energy in eV) for plate-grid separation D (a) 2 cm, (b) 4 cm, (c) 6 cm; magnetic field 69 g and gun-plate distance $L_p = 51$ cm in all cases

the grid, keeping the distance between the plate and the gun fixed at 51 cm. The plate-grid distance is changed by intervals ranging between 2–10 cm. The plate and grid currents flowing to the ground are measured by recording the potential drop across a 470 kΩ resistor and deducing the current therefrom.

It may be emphasized that the methodology of this experiment is different from that used in the earlier experiment [4] where, as was mentioned earlier, a biased grid was used that produced a secondary stream as its bias voltage was swept. The present experiment is much simpler as both the plate and the grid are grounded here and no secondary stream is possible.

Figures 2(a)–2(c) exhibit the plate and grid currents as a function of the electron energy for the plate-grid distances, 2 cm, 4 cm, and 6 cm, respectively, but for the same magnetic field value, 69 G. Taking the plot of Fig. 2(a) for the minimum plate-grid distance of 2 cm, as a reference, we notice a rather striking beatlike modification of the curve progressively with increasing separations, 4 cm and 6 cm of the grid from the plate. We notice the increase in the number of beats with increasing separation within the same sweep of the electron energy 0–500 eV. This points to an increase in the frequency of the beats with respect to electron energy sweep, with increase in the plate-grid separation. We shall see later

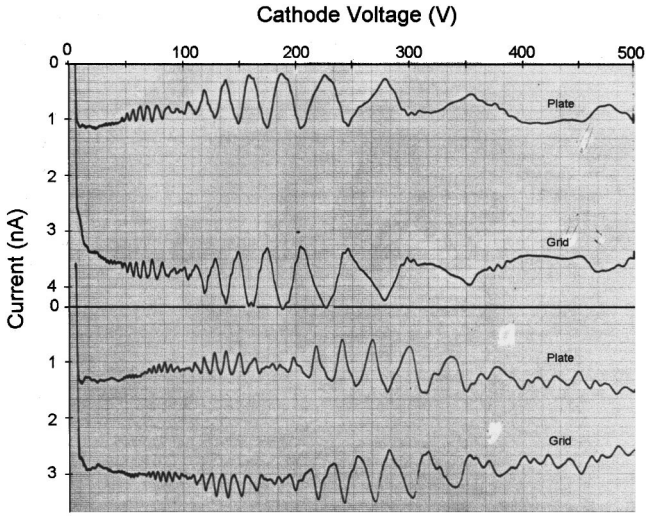

FIG. 3. Plate and grid current plots as a function of cathode voltage (electron energy in eV) for gun-grid distance $L_g = 45$ cm, (a) magnetic field $B = 69$ g, (b) $B = 135$ g.

that this dependence is in accordance with the wave algorithm.

We next consider Fig. 3, which compares the plots obtained for two different magnetic field values, $B = 69$ G and 135 G, but the same plate-grid separation of 6 cm, and the same plate-gun distance $L_p = 51$ cm, which is fixed at this value for all the plots. We again notice an increase in the number of beats with an increase in the magnetic field from 69 G to 135 G.

As one continues to increase the plate-grid separation, one gets more and more beats. Fig. 5 represents another illustrative plot for plate-grid separation, $D = 11$ cm (gun-grid distance $L_g = 40$ cm, and $L_p = 51$ cm) with a magnetic field $B = 125$ G. We see a profusion of beats in this case, both because of the larger value of D, as well as of the magnetic field.

It is clear from the above observations that the beat frequency is determined by the difference between the gun-plate distance L_p and the gun-grid distance L_g. We shall see in Sec. IV, that the frequency of the main oscillations over which the beats ride as modulation is determined by the gun-plate distance L_p. The presence of grid provides another distance L_g, between the gun and grid. The beat frequency is then found to correspond to the difference of two frequencies characterized by the two distances L_p and L_g.

As one continues to increase the plate-grid distance, and the grid crosses the midway mark between the gun and plate ($L_g \geqslant 26$ cm), one no longer has the condition appropriate for beats (which requires that $L_p \gtrsim L_g$), and the character of the plots changes entirely. Fig. 6 gives the plots for $L_g = 10$ cm. As expected, one no longer has the beats, but rather a superportion of two frequencies corresponding to the two distances L_p and L_g: the higher-frequency variation riding over the low-frequency variation, the former characterized by L_p and the latter by L_g.

Finally, one must point out the rather striking complete anticorrelation between the variations of the plate and the grid currents. This is due to the constraint that there can be

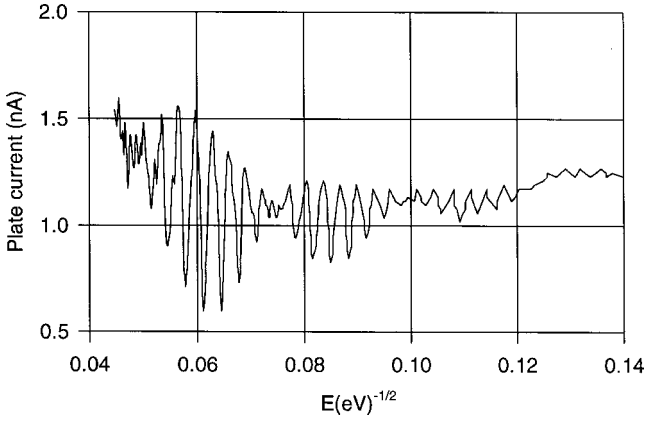

FIG. 4. Plate current plot transformed as a function of $\mathcal{E}^{-1/2}$; $\mathcal{E}$, the electron energy in elctron volts fot the plot of Fig. 3.

no transport of electrons across the magnetic field, and the current along the magnetic field must be conserved. Consequently any variation of current on the plate must be compensated for by an equal and opposite grid current. Hence the anticorrelated grid current.

III. ANALYSIS OF THE EXPERIMENTAL DATA

Having made some qualitative observations about the nature of the plots, we present now a quantitative analysis of these plots, to determine the positions of the maxima (or minima) in the plate and grid currents with respect to the electron energy and their dependence on the magnetic field B, and the appropriate distance, L_p in case of the basic higher-frequency variation in the various plots (which are modulated by the beats) and the difference $D=L_p-L_g$, for the beats.

If we recall the form of the wave function for the macroscopic matter wave $\Psi=\exp(ikx)$ with $k=\Omega/v_{\|}$, obtained in Sec. I (and also obtained independently in the Appendix) it suggests, for the positions of the interference maxima, in the energy domain a relation of the form $\Omega L=2\pi l v_{\|}(l=1,2,3...)$, with the appropriate L. Later in Sec. IV we present a detailed discussion to obtain relations of this form for the interference maxima as well as for the beats. We shall analyze the plots of Figs. 2–6 to look for relation of this

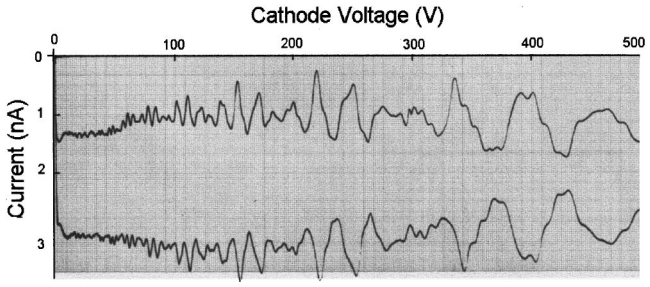

FIG. 5. Plate and grid current plot fot the gun-grid distance $L_g=40$ cm, $B=125$ g, and gun-plate distance $L_p=51$ cm.

form for the positions of the maxima.

First consider the maxima of Fig. 2(a), which with $D\equiv(L_p-L_g)=2\ \mathrm{cm}\ll L_p$ (51 cm) exhibit no beats over the range of the energy sweep (0–500 eV). The maxima should correspond to the distance $L_p=51$ cm, and described by the relation

$$\Omega L_p=2\pi l v_{\|},\quad l=1,2,3,\ldots. \tag{3}$$

To check this, we give in Table I, the energy values corresponding to the maxima of the plate current, and the corresponding values of the quantity $(\Omega/2\pi v)$ for the magnetic field used, 69 G. If this quantity for the various positions of the maxima is to fit the relation (3), then it must be an integral multiple of an appropriate common factor. In the next column, the closest such integers are identified. Using these we calculate in each case the value of L_p as required by the relation (3). In this way, we determine the measure of a distance in the experiment that has played a determining role. These values are given in the last column of Table I, and their average value $\overline{L_{ded}}=50.8$ cm is given in the footnote. This is to be compared with the actual value fixed in the experiment, namely, $L_p=51$ cm, and is in excellent agreement with it. This shows that the peaks of the plots of Fig. 2(a) are indeed well described by the relation (3), with L_p being the gun-plate distance.

Next, we want to point out that for a given magnetic field, the frequency of oscillation of the wave function with $\mathcal{E}^{-1/2}$, is proportional to the distance L_p. Considered with respect to the variation of $\mathcal{E}$ (rather than $\mathcal{E}^{-1/2}$), as is done in the

TABLE I. Energy peak positions $\mathcal{E}_l$, "quantum number" identified, l, the plate-gun distance L_{ded}, deduced from the relation, $\Omega L_{ded}=2\pi/v$, corresponding to the curve of Fig. 2(a). $B=$ ambient magnetic field, $\Omega=eB/mc$, the gyrofrequency and v, the electron beam velocity.

Peak No.	$\mathcal{E}_l$ (eV)	$k=\Omega/2\pi v$ (cm^{-1})	l	$L_{ded}=l\left(\frac{2\pi v}{\Omega}\right)$ (cm)	Peak No.	$\mathcal{E}_l$ (eV)	$k=\Omega/2\pi v$ (cm^{-1})	l	$L_{ded}=l\left(\frac{2\pi v}{\Omega}\right)$ (cm)
1	246.7	0.1975	10	50.6	6	110.0	0.2954	15	50.8
2	206.7	0.2158	11	51.0	7	96.7	0.3153	16	50.7
3	173.3	0.2356	12	50.9	8	85.6	0.3348	17	50.8
4	146.7	0.2561	13	50.8	9	76.6	0.3534	18	50.9
5	126.7	0.2756	14	50.8	10	69.0	0.372	19	51.1

Magnetic field $B=69$ g, $L_p=51$, and average $L_{ded}=50.8$ cm.

TABLE II. Energy peak positions $\mathcal{E}_l$ of beat maxima; l, the quantum number identified for the particular beat in Fig. 3; D, the grid-plate distance as required by the relation $D\Omega = 2\pi l v$; B = ambient magnetic field, $\Omega = eB/mc$, the gyrofrequency, v, the electron beam velocity, $\overline{D}$—average of D values.

Beat No.	$\mathcal{E}_l$ (eV)	$k = \Omega/2\pi v$ (cm^{-1})	l	$\mathrm{D} = l\left(\frac{2\pi v}{\Omega}\right)$ (cm)
1	55.0	0.820	5	6.1
2	83.3	0.6682	4	6.0
3	141.7	0.5103	3	5.83
4	283.0	0.358	2	5.58

Magnetic field $B = 135$ g, $D = 6$ cm, and average $\overline{D} = 5.9$ cm.

experiment, the distance L_p still characterizes the "frequency" of oscillation, but on an inverse stretched scale. Making use of this identification (frequency of oscillation with the distance L_p), we now analyze the plot of Fig. 3(b) for $B = 135$ G and $D = 6$ cm that exhibits the beats, to see if the position of the maxima of the beats can be described by a relation of the above form. In Table II we tabulate the positions of the beat maxima in energy and the values of the quantity $(\Omega/2\pi v)$ in the same way as was done in Table I, for the plot of Fig. 2(a). The last column gives for each case, the value of the distance D which corresponds to the relation.

$$\Omega D = 2\pi l v \quad (l = 1,2,3, \ldots). \tag{4}$$

The average value of D so obtained from the experimental data [with the use of the relation (4)] $\overline{D} = 5.9$ cm is given in the footnote. We see that this value is indeed close to the difference $(L_p - L_g)$ of the two distances L_p and L_g, namely, $(L_p - L_g) = 6$ cm used in this particular run [plot of Fig. 3(b)]. It shows that the beat frequency deduced from the plot does correspond to the frequency characterized by the difference $(L_p - L_g)$, that is the difference of two "frequencies" present in the system, characterized by the distances L_p and L_g, just as it happens in any wave phenomena.

It may be specifically emphasized that the beat frequency being equal to the difference between the two prevailing frequencies in the system is a specific consequence of the wave formalism, whereby the intensity or the probability current is obtained as a magnitude squared of the sum of the two amplitudes of the interfering waves with the two frequencies. In fact, it will be shown in the next section how it comes about in the present situation. On the other hand, the sum of two oscillating particle sources with closely spaced frequencies ω_1 and ω_2 will also produce beats, but with only half the frequency of the difference, $\omega_b = 1/2(\omega_1 - \omega_2)$, rather than with $(\omega_1 - \omega_2)$ as with waves. It may, therefore, be mentioned that the observation of beats with the right frequency constitutes a crucial test for the existence of the wave picture, since there will be little room now for the possibility of understanding these results in terms of the classical particle picture as was suggested [5,6] for the earlier results.

We thus arrive at a very important conclusion through the confirmation of the existence of beats with the right frequency, that what we have observed in these experiments is indeed a manifestation of matter wave phenomena in the macrodomain of a few centimeters. This, it must be emphasized, is an extraordinary result because matter waves have been observed in the macrodomain with all the appropriate characteristics. Before we discuss the wave algorithm as applied to this system in the next section, we shall present an analysis of Fig. 6, which corresponds to widely different values of the distances L_p and L_g, and, therefore, of the corresponding frequencies. Figure 6 corresponds to $L_p = 51$ cm, $L_g = 10$ cm. As expected, there are no beats now, but merely a simple superposition of two frequencies, the higher-frequency oscillation corresponding to $L_p = 51$ cm, riding over the low-frequency variation corresponding to $L_g = 10$ cm. We shall see in the next section how this too comes about.

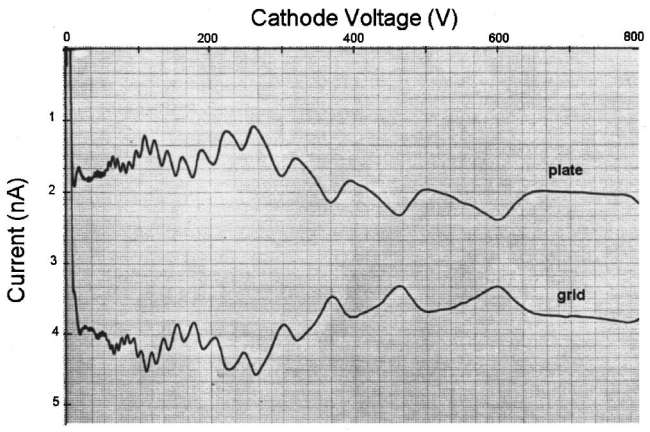

FIG. 6. Plate and grid current plot for the gun-grid distance $L_g = 10$ cm, and magnetic field $B = 69.02$ g.

We shall analyze here only the low frequency to see what value of L do the maxima of the oscillation yield if they are to fit in a relation of the form $\Omega L = 2\pi l v$. Following the same procedure as before, we tabulate in Table III the various quantities as indicated there, calculating the values of L in each case, given in the last column. The average $\overline{L}$ value of these calculated L values, $\overline{L} = 10.1$ cm shows that it does

TABLE III. Energy peak position $\mathcal{E}_l$ of the slowly varying part of Fig, 5. l, the quantum number identified for the peaks; L_g, the anode-grid distance as required by the relation $L_g\Omega = 2\pi l v$; $\Omega = eB/mc$, the gyrofrequency; B, the ambient magnetic field, $\overline{L_g}$, the average value of L_g,

$\mathcal{E}_l$ (eV)	$\Omega/2\pi v$ (cm^{-1})	l	$L = l\frac{2\pi v}{\Omega}$ (cm)	$\overline{L_g}$ (cm)
38.33	0.50	5	10.0	
60.0	0.40	4	10.0	10.1
105.0	0.302	3	9.9	
256.7	0.19	2	10.5	

Magnetic field $B = 69.2$ g, $L_g = 10$ cm, and Average $\overline{L} = 10.1$ cm.

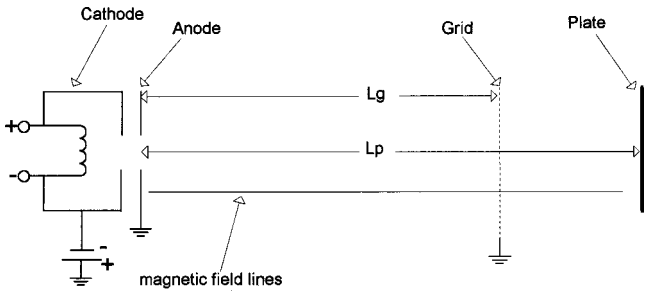

FIG. 7. Schematics of the experimental arrangment indicating the various relevant distances, L_p, L_g, etc.

correspond to the gun-grid distance $L_g = 10\,\mathrm{cm}$, which was chosen to be so for this particular run (Fig. 6). We, therefore, conclude that the low frequency in this limit ($L_g \ll L_p$) corresponds to the gun-grid distance L_g.

IV. THE WAVE ALGORITHM FOR THE PRESENT EXPERIMENT

We now present the wave algorithm that follows from the Schödinger-like formalism of Refs. [1], [2]. We shall apply this formalism to the above experiment and shall show how the experimental results can be understood in terms of the former.

We recall from Sec. I (as well as from the Appendix) that the wave function for the progressive macroscopic matter wave associated with electron motion along a magnetic field is given, for the mode number $n=1$, by $\Psi(1)=\exp(ikx)$, where $k=\Omega/v$, and v the electron velocity parallel to the magnetic field (the subscript ''parallel'' is dropped). Other waves corresponding to the mode number $n=2,3,...$, may also be present, for which the wave function is $\Psi(n)=\exp(inkx)$, but the mode $n=1$ is the most dominant. We shall discuss later that the experimental curves do imply the existence of the other modes through the presence of higher harmonics in their periodic variation. We shall, however, consider only the $n=1$ mode at the present time.

Consider now the experimental arrangement as shown schematically in Fig. 7. Electrons from an electron source *S*, are injected with a velocity almost parallel to the magnetic field. *P* and *G* denote the plate and grid respectively (both grounded), at distances L_p and L_g from the source. Let x be the field point within the plate just behind the plate surface, where the ''detection'' is assumed to occur. The total wave amplitude at x is comprized of a sum of three contributions: (i) one corresponding to the particles arriving directly from the source *S*, $\gamma\exp(ikx)$, (ii) another one corresponding to the particles arriving after being scattered off the grid so that the grid acts as a secondary source for them, the corresponding wave amplitude being, $\alpha\exp[ik(x-L_g)]$ and (iii) a third one from particles arriving after being scattered off the plate surface, their amplitude likewise being, $\beta\exp[ik(x-L_p)]$. Thus the wave amplitude at x (a point just behind the plate surface) is

$$\psi_p(x)=\alpha e^{ik(x-L_g)}+\beta e^{ik(x-L_p)}+\gamma e^{ikx}, \tag{5}$$

where α is the coefficient of the forward scattering amplitude at the grid, β that of the forward scattering amplitude at the plate surface, and γ is the amplitude of the direct unscattered wave arriving at the point x. It would be desirable to have an idea about the relative magnitudes of the various coefficients α, β, and γ. But at the moment we do not have that information. However, what is important at present is the development of the wave algorithm to check the experimental observations against it even if qualitatively. We emphasize that these observations represent paradigm according to which, as mentioned already, there exist matter wave manifestations in the macrodomain for charged particles propagating along magnetic field.

If ψ_g is the amplitude for the absorption of the wave at the grid, then from the conservation of total probability current in this one-dimensional case, we have

$$|\psi_g|^2+|\psi_p|^2=1, \tag{6}$$

where $|\psi_p|^2$ is proportional to the probability current recorded by the plate, and clearly transmitted past the grid. Since the transmitted current must have a significant forward scattered component, we write approximately $\alpha=\alpha_o|\psi_p|^2$. We then have

$$\psi_p=\alpha_o|\psi_p|^2e^{ik(x-L_g)}+\beta e^{ik(x-L_p)}+\gamma e^{ikx}, \tag{7}$$

whence taking magnitude squared, we get

$$\begin{aligned}|\psi_p|^2=&[1-2\alpha_o\gamma\cos kL_g-2\alpha_o\beta\cos k(L_p-L_g)]^{-1}\\&\times[\gamma^2+\beta^2+2\beta\gamma\cos kL_p],\end{aligned} \tag{8}$$

where we have neglected $\alpha_o^2|\psi_p|^4$ as being small compared to the rest of the terms.

Expanding the denominator in the expression (8) we obtain

$$\begin{aligned}|\psi_p|^2\approx&(\beta^2+\gamma^2)+2\beta\gamma\cos kL_p+2\alpha_o(\gamma^2+\beta^2)[\gamma\cos kL_g\\&+\beta\cos k(L_p-L_g)]+4\alpha_o\beta\gamma\cos kL_p[\gamma\cos kL_g\\&+\beta\cos k(L_p-L_g)]\\\approx&\beta^2+\gamma^2+2\beta\gamma\cos kL_p+2\alpha_o\gamma(\beta^2+\gamma^2)\cos kL_g\\&+2\alpha_o\beta(\beta^2+2\gamma^2)\cos k(L_p-L_g)\\&+2\alpha_o\gamma^2\beta\cos k(L_p+L_g)\\&+4\alpha_o\beta^2\gamma\cos k(L_p-L_g)\cos kL_p,\end{aligned} \tag{9}$$

where we have changed the $\cos kL_p\cos kL_g$ term into $1/2[\cos k(L_p-L_g)+\cos k(L_p+L_g)]$. There are then various kinds of terms. The presence of the term $\cos kL_p$ arises only through the coefficients β or γ, which represent the scattering off the plate surface ($\sim\beta$) and the coefficient of the unscattered wave amplitude ($\sim\gamma$). All the other terms involve α_o, that is the coefficient of the wave amplitude scattered off the grid. We see that while the first four terms of Eq. (9) represent variation with respect to k with ''frequencies,'' respectively, L_p, L_g, (L_p-L_g) and (L_p+L_g), the last term represents a modulation with the frequency (L_p-L_g) of the

variation with respect to k with the frequency L_p. The frequency (L_p-L_g) represents a beat frequency between the two frequencies L_p and L_g present in the system as these two distances. It may be emphasized that the beat frequency equal to the difference (L_p-L_g) arises as a consequence of the wave algorithm whereby the intensity is obtained as $|\psi_p|^2$, (modules squared of the wave amplitude ψ_p at the plate). We consider three cases: (A) $L_p \approx L_g$; $(L_p-L_g)=\Delta \ll L_p$, (B) $L_p \geqslant L_g$; $\Delta/L_p \leqslant 0.2$ (say), and (C) $L_g \ll L_p$.

Case (A): $L_g \approx L_p$; $L_p-L_g=\Delta \ll L_p$. If we consider the limiting case when the grid is very close to the plate, so that $(L_p-L_g)\equiv\Delta \ll L_p$, then we get

$$|\psi_p|^2=\beta^2+\gamma^2+2\alpha_o\beta[\beta^2+2\gamma^2] +[2\beta\gamma+2\alpha_o\gamma(3\beta^2+\gamma^2)]\cos kL_p +2\alpha_o\beta\gamma^2\cos 2kL_p. \quad (10)$$

This gives a variation with $k(\equiv\Omega/2\pi v)$ of $|\psi_p|^2$, which is characterized by the ''frequency'' determined essentially by the gun-plate distance L_p and corresponds to the plot of Fig. 2(a), with the value of $L_p=51$ cm, and the magnetic field $B=69$ G. Using these values, the various energy peaks in the plot of Fig. 2(a) have been characterized through the relation $\Omega L_p=2\pi l v$ by the ''quantum numbers'' l. These are presented in Table I corresponding to the different peaks as allowed energy values. It is thus seen that the observed energy peaks (''allowed'' values) do correspond to the relation $\Omega L_p=2\pi l v$, which is obtained using the wave algorithm with the wavelength $\lambda=2\pi v/\Omega$. For the value of $B=69$ G and energy $\mathcal{E}=200$ eV (say), $\lambda\approx 4.6$ cm. Thus the electrons of energy 200 eV, behave like an effective de Broglie-like wave of wavelength $\lambda\approx 4.6$ cm in a magnetic field of 69 G, which is of a rather macroscopic dimensions and is independent of the Planck quantum.

It may further be noticed that, the grid and plate currents are found to be anticorrelated in all cases. This, as remarked already, is a reflection of the total current conservation along the magnetic field as expressed by the relation (6). Any maxima-minima that the plate current may exhibit as a consequence of the interference effects, must be compensated for in the form of complementary grid current that we find to be the case in all the plots of Figs. 2, 3, and 6. In our earlier experiment [4] such a complementary current appeared on the anode as the grid and plate currents there, because of the particular nature of that experiment, were positively correlated.

Case (B): $L_p \geqslant L_g$, $(1-L_g/L_p)=\delta \leqslant 0.2$ (say). This case is the one that is appropriate for beats. Using the inequality $\delta \ll 1$, expression (9) gives in this case

$$|\psi_p|^2=(\beta^2+\gamma^2)+[2\beta\gamma+2\alpha_o\gamma(3\beta^2+\gamma^2)] \times\cos kL_p+2\alpha_o\beta\gamma^2\cos 2kL_p +2\alpha_o\beta(\beta^2+2\gamma^2)\cos k(L_p-L_g) +2\alpha_o\beta\gamma(2\beta+\gamma)\cos k(L_p-L_g)\cos kL_p, \quad (11)$$

where the last term represent the modulation of the oscillating term $\cos kL_p$, with the beat frequency (L_p-L_g).

The analysis of the plots in Fig. 3 as presented in Table II, shows that the beat frequency is indeed characterized by the difference (L_p-L_g), precisely what is required by the expression (11). Since the latter expression for the probability current at the plate is derived assuming the wave algorithm with the wave number $k=\Omega/v$, [the various orders $l=5,4,3,2$ identified in Table II that correspond to the relation $k(L_p-L_g)=2\pi l$, describing the maxima in Eq. (10)] it follows that the observed beat structure does conform to a wave behavior with the wavelength $\lambda=2\pi v/\Omega$. We also note the fast variation $\cos kL_p$, which is modulated by $\cos k(L_p-L_g)$, and which is characterized by the length L_p in the expression, also agrees with the observations.

We note from here that in terms of the variation with the wave number k, the lengths L_p, and (L_p-L_g) act as a ''frequencies.'' So if the various Figs. 2(a)–2(c) and 3(a,b) are replotted as a function of $\mathcal{E}^{-1/2}$, which is proportional to k, $[k=\Omega(2\mathcal{E}/m)^{-1/2}]$, rather than what they are (as a function of $\mathcal{E}$), then the various maxima, including the beat maxima would be found to be equally spaced, with the interpeak interval being inversely proportional to the distance L_p or (L_p-L_g), the latter one in the case of beats, while the former for the main interference maxima and minima.

We have done just that for the plot of Fig. 3(b). The replotted curve that is obtained after digitizing the plot of Fig. 3(b) manually and converting the data points in terms of $\mathcal{E}^{-1/2}$, leads to the plot of Fig. 4. As expected, we do find the maxima including those of the beats equidistant on the $\mathcal{E}^{-1/2}$ scale.

Case (C): $L_g \ll L_p$. We next consider the case when the gun-grid distance L_g is much less than L_p. In this case we obtain

$$\begin{aligned}|\psi_p|^2&=\beta^2+\gamma^2+2\beta\gamma\cos kL_p \\ &\quad+2\alpha_o(\gamma^2+\beta^2)[\gamma\cos kL_g+\beta\cos k(L_p-L_g)] \\ &\quad+4\alpha_o\beta\gamma\cos kL_p[\gamma\cos kL_g+\beta\cos k(L_p-L_g)] \\ &\approx\beta^2+\gamma^2+2\alpha_o\beta^2\gamma(1+\cos 2kL_p) \\ &\quad+2\alpha_o(\gamma^2+\beta^2)\gamma\cos kL_g \\ &\quad+[2\beta\gamma+2\alpha_o\beta(3\gamma^2+\beta^2)]\cos kL_p. \quad (12)\end{aligned}$$

We see that in this limit $(L_g \ll L_p)$, $|\psi_p|^2$ is a sum of three terms, going as $\cos kL_p$, $\cos kL_g$, and $\cos 2kL_p$. The first two together yield a fast variation $\cos kL_p$ riding over a slow variation $\cos kL_g$, precisely the kind of variation exhibited by the plot of Fig. 5. The term going as $\cos 2kL_p$ represents only a second harmonic of $\cos kL_p$, which may well be present in the variation of periodicity characterized by the distance L_p.

Again the plot of Fig. 6 is well represented by the expression of the form (12), which is obtained from the wave algorithm based on the formalism of Refs. [1], [2] in the limit $L_g \ll L_p$. Thus taken all the cases (A), (B), and (C) together, the wave algorithm given here appears to describe the plots of Figs. 2, 3, 4, and 6. It must also be mentioned that it has not been found possible for the authors to find any other

explanation for these plots in terms of the equation of motion-initial value paradigm (referred to as the ''standard paradigm''). We refer to the discussion in Ref. [4] to rule out any possible plasma physical explanation, essentially because of the very low beam current (~nA) used and high vacuum ($\sim 5\times 10^{-7}$ Torr) employed.

V. SUMMARY AND DISCUSSION

We have presented in this paper experimental observations on the ''beats'' as a conclusive evidence for the existence of matter wave phenomena in the macrodomain, for electrons moving along a magnetic field. The ''beat frequency'' agrees entirely with the expectation of the wave formalism, being equal to the difference of the closely spaced frequencies of the two interfering waves. The ''frequencies'' correspond here to gun-plate and gun-grid distances, L_p and L_g, respectively, and the ''beats'' have been found in the experiments to have the frequency corresponding to the difference $(L_p - L_g)$.

The earlier experiment [4] had also exhibited the existence of discrete energy band structures that were shown there to be a manifestation of matter wave phenomena. The frequency of variation of the plate current was characterized by just one distance in the experiment, the gun-plate distance. However, as was mentioned in Sec. III, these observations do permit some room for the possibility of being explained [5,6], in terms of the classical charged particle trajectories, even though the authors of Ref. [6] have themselves noted their proposed mechanism to be not entirely adequate to explain the depth of the observed modulation.

The importance of the observations of beats with the right frequency (equal to the difference of the frequencies of the two interfering waves, which is determined by a wave formalism), lies in the fact, that these beats (with this frequency) are a definite indicator of the wave formalism being at play to govern the dynamics of the electrons. Such beats cannot be explained in terms of the particle picture.

We thus conclude that taken together the results obtained earlier [4] on the existence of discrete energy band structures in the transmission of electrons along a magnetic field, and those reported in this paper on the existence of beats modulating this band structure, constitute a convincing evidence for the existence of a probability wave in the macrodomain associated with the motion of electrons along a magnetic field.

The probability matter wave has the wave function of the form $\Psi(1)=\exp[2\pi i x/\lambda]$, with $\lambda = 2\pi v/\Omega$, v being the electron velocity along the magnetic field, and as shown in Sec. IV, the discrete energy band structure as well as the ''beats'' are a consequence of one-dimensional interference effects with the wave function of the above form, and with a wavelength typically $\lambda \sim 5$ cm, which is clearly in the macrodomain. These are extraordinary results by any account, because matter waves with such macroscopic wave lengths (~5 cm) have not been either conceived or observed before, even if in the limited context of charged particle dynamics along a magnetic field.

Needless to say, these results are clearly contrary to the expectations of the classical Lorentz equation of motion that governs the dynamics of charged particles in the classical macrodomain. The question naturally presents itself as to what the relationship is between the dynamics determined by the Lorentz equation, and the one governed by the Eqs. (1) and (2), which have predicted these effects. This will be taken up in a subsequent study.

One may ask another interesting question. Is the observation of macroscopic matter waves as demonstrated above entirely peculiar to the system of charged particles in a magnetic field? The answer is, rather interestingly, in the negative. In fact, the author (Varma) has pointed out [7] other possible physical systems (such as atoms and molecules in their highly-excited internal states), which could exhibit matter waves in the macrodomains and mesodomains.

APPENDIX: A QUANTUM MECHANICAL JUSTIFICATION OF THE NON-PLANCKIAN MACROSCOPIC MATTER WAVE BEHAVIOR OF ELECTRONS ALONG A MAGNETIC FIELD

A charged particle in a magnetic field in the classical mechanical domain corresponds in quantum mechanics to the particle in a Landau level with a large quantum number. If E_ν represent the energy of a Landau level, so that

$$E_\nu = \left(\nu + \frac{1}{2}\right)\hbar\Omega, \tag{A1}$$

where $\Omega = eB/mc$ is the gyrofrequency in the magnetic field B, then $\nu \gg 1$ corresponds to the classical limit, and $\nu\hbar = \mu$ defines the gyroaction that appears in Eq. (2) of the formalism of Ref. [1]. Let χ_ν represent the Landau eigenfunctions that are essentially the harmonic oscillator wave functions. Consider now the propagation of an electron beam along a magnetic field in such a set of Landau levels with $\nu \gg 1$. Let there be a scatterer in the path of the electron beam such as a small obstacle, like the wires in a grid that the electron beam may pass through. The anode of the electron gun through which the electron beam passes in the process of acceleration may also act as a scatterer. The scattering, assumed to be elastic, may kick the electron from the Landau level ν to $\nu \pm n$, where $\nu \gg n > 1$. If $\tilde{H}$ be the perturbation Hamiltonian that describes the scattering, then the transition amplitude for this process

$$\alpha_\nu^n \equiv \langle \nu - n|\overline{H}|\nu\rangle = \int d\xi\, \chi_{\nu-n}\tilde{H}\chi_\nu, \tag{A2}$$

ξ being the coordinate normal to the magnetic field. If φ_ν represents the complete wave function of the particle in a magnetic field including the plane wave along the magnetic field (assumed homogeneous), we have

$$\varphi_\nu = \chi_\nu(\xi)e^{i\kappa_\nu x}, \tag{A3}$$

where

$$\kappa_\nu = \frac{1}{\hbar}[2m(E-\nu\hbar\Omega)]^{1/2}, \tag{A4}$$

where x is the coordinate along the magnetic field, and E is the total energy of the particle. The transition amplitude including the eigenfunction along the field

$$\begin{aligned}\beta_\nu^{(n)} &\equiv \langle \nu-n, \kappa_{\nu-n}|\tilde{H}|\nu,\kappa_\nu\rangle \\ &= \int d\xi\, \varphi^*_{\nu-n}(\xi)\tilde{H}\varphi_\nu \\ &= = \alpha_\nu^{(n)} e^{i(\kappa_\nu-\kappa_{\nu-n})x}.\end{aligned} \tag{A5}$$

Now making use of the assumption $n \ll \nu$, we expand $\kappa_{\nu-n}$ around κ_ν, using the expression (A4), we get

$$\kappa_\nu - \kappa_{\nu-n} \simeq n\frac{\partial\kappa_\nu}{\partial\nu} = n\Omega\left[\frac{2}{m}(E-\nu\hbar\Omega)\right]^{-1/2} = \frac{n\Omega}{v}, \tag{A6}$$

where

$$v = \left[\frac{2}{m}(E-\nu\hbar\Omega)\right]^{1/2},$$

is the velocity along the magnetic field. The transition amplitude β_ν^n is then given by

$$\beta_\nu^{(n)} = \alpha_\nu^n e^{i(n\Omega/v)x}, \tag{A7}$$

so that it corresponds to a wave with the wave number

$$k_n = \frac{n\Omega}{v}, \tag{A8}$$

which for $n=1$, gives essentially the wavelength $\lambda_{\text{eff}} = 2\pi v/\Omega$ and is clearly independent of $\hbar$. It is, therefore, this transition amplitude (A7) that is responsible for the non-Planckian wave behavior for the motion along the magnetic field that have been reported here as well as earlier in Ref. [4].

Note that $n \geqslant 2$ in Eq. (A7) would correspond to the higher harmonics of the fundamental wave corresponding to $n=1$. An examination of the plots of the various Figs. 2–5 would reveal that higher harmonics must be present. These higher harmonics, it may be pointed out, correspond to the Eq. (1) for higher values of the modes $n(n \geqslant 2)$. Thus the formalism of Refs. [1,2] does contain the higher harmonics as well.

[1] R. K. Varma, Phys. Rev. E **64**, 036608 (2001).
[2] R. K. Varma, Phys. Rev. A **31**, 3951 (1985).
[3] T. G. Northrop, *Adiabatic Motion of Charged Particles* (Interscience, New York, 1963).
[4] R. K. Varma and A. M. Punithavelu, Mod. Phys. Lett. A **8**, 167 (1993); **8**, 3823 (1993).
[5] C. S. Unnikrishnan and C. P. Safvan, Mod. Phys. Lett. A **14**, 479 (1999).
[6] A. Ito and Z. Yoshida, Phys. Rev. E **63**, 026502 (2001).
[7] R. K. Varma, Phys. Rev. A (to be published).